REMARKS

Claims 1-28 and 33-38 are pending in the subject application. By this Amendment, Applicants have amended claims 1, 11, 21, and 34. Accordingly, claims 1-28 and 33-38 are pending in the subject application.

Support for amended claim 1, 11, 21, and 34 may be found, inter alia, on page 2, lines 7 to 10; page 2, line 33 to page 3, line 4; page 9, lines 27-33; and page 15, line 2 to page 16, line 10 of the specification.

Rejections Under 35 U.S.C. § 102(e)

On page 3 of the February 23, 2004 Office Action the Examiner rejected Claims 1-4, 6, 12, 13, 21-23, 33, 34 and 36-38 under 35 U.S.C. 102(e) as allegedly anticipated by Schultz et al., (US 6,180,415).

The Examiner alleged that Schultz et al. disclose a method for detecting the presence of and information about, a target having a molecular feature of interest (col 5 and 6, col 34, line 6 - col 35 line 33). The Examiner alleged that Schultz et al. disclose contacting the target with one or more plasmon resonant particles ("PRE's" or "PRP's") (which the Examiner characterized as labels) having surface localized molecules to produce an interaction between the molecular feature and the localized molecules. The Examiner alleged that Schultz et al. disclose that the target contains a ligand-binding site, and the surface localized molecule is a ligand capable of forming a ligand/ligand-binding complex (col 5, lines 60-67). The Examiner alleged that Schultz et al. disclose that the PRE's can accept pulses between 5 to 500 femtosecond for driving second harmonic generation processes. The Examiner alleged that Schultz et al. disclose contacting a surface with these PRE's thereby creating an interface at the surface which has target attached thereto wherein the target is not labeled with a non-linear label wherein the target is not detectable at the interface using a surface selective technique

and wherein the target is labeled when the PRE comprising the ligand partner for the target attaches to the target and measuring a change in nonlinear optical light at the interface in the presence of the labeled target using a nonlinear optical technique. The Examiner alleged that Schultz et al. disclose that the PRE's can be used for cell sorting. The Examiner alleged that Schultz et al. disclose analyzing a cell type expressing a particular surface antigen using a particular PRE probe (col 49, lines 55-67).

Further, the Examiner alleged that with respect to second harmonic active-label as recited in the instant claims in the specification on page 2, lines 19-23 the Applicant defines that second harmonic active-labels are second harmonic-active moieties which can be attached to a molecule of interest that is not second harmonic active and Applicant further defines (page 8, lines 6-11) that a second harmonic refers to a frequency of light that is twice the frequency of a fundamental beam of light and that a second harmonic-active moiety is a substance which when irradiated with a fundamental beam of light generates a second harmonic of the fundamental. The Examiner alleged that Schultz et al., disclose that the PRE's (labels) can accept pulses between 5 to 500 femtosecond for driving second harmonic generation. On this basis the Examiner alleged that Schultz et al. disclose second harmonic labels.

The Examiner stated that Applicants' arguments filed January 23, 2004 have been fully considered but they are not persuasive.

The Examiner noted Applicants' argument on page 13 of the February 23, 2004 Office Action, that Schultz et al. do not disclose a method comprising "using a surface selective technique," as recited in Applicants' claims. Specifically, only noncentrosymmetric second harmonic generators can be used with a surface selective technique as recited in Applicants' claims. See, for example, page 2, line 7-13 of the subject specification as well as **Exhibits A-D** submitted

with Applicants' January 23, 2004 Amendment. The Examiner agreed that with Applicants' contention that the plasmon resonant particles "PRE's" of Schultz et al. can be "spherical." The Examiner alleged, however, that Schultz et al. also teach that the PRE's can be non-spherical.

In response to Applicants' argument that the references fail to show certain features of Applicants' invention, the Examiner alleged that the features upon which Applicants rely (i.e., only noncentrosymmetric second harmonic generators can be used) are not recited in the rejected claim(s). The Examiner cited *In re Van Geuns*, 988 F.2d 1181, 26 USPQ2d 1057 (Fed. Cir. 1993).

In response, Applicants have clarified claim 1 and 34 to recite that the "second harmonic-active label ... is hyperpolarizable and contributes to a net orientation at the interface." Applicants have also amended claim 21 to recite a second harmonic-active label, "which is hyperpolarizable and contributes to a net orientation at an interface."

Furthermore, Applicants' point out that although the PREs of Schultz et al. "can accept" light pulses that can also be used to drive second harmonic-active labels, the PRE's scatter the light at the same wavelength as the light shone on them. On the other hand, Applicants' second harmonic-active labels scatter the light at one-half (½) the wavelength shone on them. It is clear from Schultz et al. and related articles, e.g. Schultz et al., "Single-target Molecule Detection With Nonbleaching Multicolor Optical Immunolabels," *PNAS*, February 1, 2000, Vol. 97, No. 3, pp. 996-1001, attached as **Exhibit A**, that PRE's (also referred to as PRP's) do not generate a second harmonic.

The statement by Schultz et al. that "they [PRE's] can accept" merely means one can use the same ultrashort pulses used to drive the nonlinear processes for also driving the *elastic* plasmon

resonance process. Schultz et al., do not anywhere state that the PREs can be used for second harmonic or higher order detection-based assays, i.e., generation and detection of the second harmonic or higher order beams. In addition, Schultz et al. do not describe the absolute requirement of non-centrosymmetry for second harmonic generation or any intention to use the PREs for second harmonic generation in an assay.

Applicants reiterate that they are claiming a method which is neither taught nor suggested by Schultz et al. Nowhere do Schultz et al. teach or suggest using a surface selective technique, i.e. a technique requiring the labels to have "hyperpolarizability and a net orientation at the interface," as pointed out on page 2, lines 9-10, and on page 2, line 33 to page 3, line 4 of Applicants' specification, and now recited in the amended claims.

Accordingly, Schultz et al. do not anticipate Applicants' claimed invention, and this rejection should be withdrawn. Furthermore, nothing in Schultz et al. suggests or motivates Applicants' claimed invention.

Rejections Under 35 U.S.C. § 103(a)

On Page 5 of the February 23, 2004 Office Action, the Examiner rejected Claims 2, 7, 8, 27 and 28 under 35 U.S.C. 103(a) as alledgedly unpatentable over Schultz et al. in view of Quinn et al.

The Examiner referred to the alleged teachings of Schultz et al. above.

The Examiner acknowledged that Schultz et al. differ from the instant invention in failing to specifically state that the surface selective technique is second harmonic generation.

The Examiner alleged that Quinn et al. disclose second harmonic generation and sum-frequency generation techniques utilized with second harmonic labels for detecting molecules of interest.

The Examiner alleged that although Schultz et al. do not specifically disclose the use of second harmonic generation as the surface selective technique, it would have been obvious to one or ordinary skill in the art to use a surface selective technique such as taught by Quinn et al. with the second harmonic label of Schultz et al. because Schultz et al. specifically teach that their labels can be used in second harmonic generation processes (col 13, lines 57-60.)

The Examiner stated that Applicants' arguments filed January 23, 2004 have been fully considered but they are not persuasive.

The Examiner noted Applicants' argument that Schultz et al. do not teach or suggest using a surface selective technique, i.e. a technique requiring "hyperpolarizability and a net orientation at the interface,". In response to Applicants' argument that the references fail to show certain features of Applicants' invention, the Examiner alleged that the features upon which Applicants rely (i.e., hyperpolarizability and a net orientation at the interface) are not recited in the rejected claim(s).

In response, as discussed above, Applicants have clarified claim 1 and 34 to recite that the "second harmonic-active label ... is hyperpolarizable and contributes to a net orientation at the interface." Applicants have also amended claim 21 to recite a second harmonic-active label, "which is hyperpolarizable and contributes to a net orientation at an interface."

Furthermore, as discussed above, Schultz et al. do not teach or suggest all the claim limitations of the instant application. As noted above, Schultz et al. do not anywhere teach or suggest that the PREs can be used for second-harmonic or higher order detection-based assays, i.e. generation and detection of the second harmonic or higher order beams. In addition, Schultz et al.

do not teach or suggest the absolute requirement of non-centrosymmetry for second harmonic generation or any intention to use the PREs for second harmonic generation in an assay.

As previously addressed in the January 23, 2004 Amendment and accepted by the Examiner, Applicants' claims recite subject matter that is patentable over Quinn et al. Specifically, Applicants' recitation that an unlabeled molecule at the interface would be undetectable using a given surface selective technique clearly distinguishes Applicants' claims from Quinn et al.

Accordingly, Applicants respectfully request that the Examiner reconsider and withdraw the rejections under 35 U.S.C. §103 over Schultz et al. in view of Quinn et al. set forth in the February 23, 2004 Office Action.

In Sections 5 to 11 of the February 23, 2004 Office Action, the Examiner rejected Claims 5, 9-11, 14-20, 24, 25, 26, and 35 under 35 U.S.C. 103(a) as allegedly unpatentable over Schultz et al. and each of the following secondary references: Mattingly et al., (US 5,145,790); Buechler et al., (US 6,194,222); Wang et al., (US 5,696,157); Eisenthal et al., (Photophysics of liquid interfaces by Second Harmonic Spectroscopy, J.Phys. Chem 1996, 100, Vol. 31, 12997-13006); Conboy et al., (J. Chem. 1994, 98, 9688-9692); Eisenthal et al., (US 6,055,051); and Tadano et al., (US 5,962,248).

In response, as discussed above, Schultz et al. do not teach or suggest all the claim limitations of the instant application. Schultz et al., alone or in combination with the secondary references, do not teach or suggest Applicants' invention as recited in the claims because the deficiencies of Schultz et al. are not remedied by the secondary references.

Accordingly, Applicants respectfully request that the Examiner reconsider and withdraw each of the rejections under 35 U.S.C. §103 over Schultz et al. in view of the secondary references.

Provisional Double Patenting

On page 12 of the February 23, 2004 Office Action the Examiner provisionally rejected Claims 1-28 and 33-38 under the judicially created doctrine of obviousness-type double patenting as being unpatentable over claims 1-17, 19, 24-49, 56-113, 131 and 132 of copending Application No. 09/907,035. The Examiner alleged that although the conflicting claims are not identical, they are not patentable distinct from each other because both sets of claims are drawn to methods for detecting molecules at an interface using similar method steps. The Examiner alleged that the instantly recited claims recite a second harmonic-active label while the 09/907,035 claims recite non-linear labels. The Examiner alleged that it is obvious to one skilled in the art that the non-linear labels encompass the second harmonic-active label.

The Examiner alleged that Applicants' arguments filed January 23, 2004 have been fully considered but they are not persuasive.

The Examiner noted that with respect to the Double Patenting rejection, Applicants argued that because all other rejections of the subject applications have been overcome, Applicants' requested that the Examiner issue the subject application pursuant to M.P.E.P. 804(1) (E). The Examiner alleged that this is not found persuasive because Applicants had not overcome the rejections of the claims as stated above and therefore, the double patenting rejection is maintained.

In response, because all other rejections of the subject applications have been overcome as discussed above, Applicants

again respectfully request that the Examiner issue the subject application pursuant to M.P.E.P. § 804(I)(B), which guides that:

> The "provisional" double patenting rejection should continue to be made by the examiner in each application as long as there are conflicting claims in more than one application unless that "provisional" double patenting rejection is the only rejection remaining in one of the applications. If the "provisional" double patenting rejection in one application is the only rejection remaining in that application, the examiner should then withdraw that rejection and permit the application to issue as a patent, thereby converting the "provisional" double patenting rejection in the other application(s) into a double patenting rejection at the time the one application issues as a patent.
>
> If the "provisional" double patenting rejections in both applications are the only rejections remaining in those applications, the examiner should then withdraw that rejection in one of the applications (e.g., the application with the earlier filing date) and permit the application to issue as a patent. The examiner should maintain the double patenting rejection in the other application as a "provisional" double patenting rejection which will be converted into a double patenting rejection when the one application issues as a patent. (Emphasis added).

Furthermore, the allegedly conflicting claims in U.S. Serial No. 09/907,035 are also subject to being amended to the point of no longer being conflicting.

In conclusion, Applicants respectfully submit that the amendment of the claims and the remarks herein overcome the rejections under 35 U.S.C. §§ 102(e) and 103, leaving only the *provisional* double patenting rejection. However, pursuant to M.P.E.P. §804(I)(B), the

provisional rejection should be withdrawn, allowing the subject application to proceed to issuance.

If a telephone interview would be of assistance in advancing prosecution of the subject application, Applicants' undersigned attorney invites the Examiner to telephone him at the number provided below.

No fee, other than the fifty-five dollar ($55.00) fee for a one-month extension of time, a check for which is enclosed, is deemed necessary in connection with the filing of this Amendment. However, if an additional fee is required, authorization is hereby given to charge the amount of any such fee to Deposit Account No. 03-3125.

Respectfully submitted,

Gary J. Gershik

John P. White
Registration No. 28,678
Gary J. Gershik
Registration No. 39,992
Attorneys for Applicants
Cooper & Dunham LLP
1185 Avenue of the Americas
New York, New York 10036
(212) 278-0400

I hereby certify that this correspondence is being deposited this date with the U.S. Postal Service with sufficient postage as first class mail in an envelope addressed to:
Commissioner for Patents
P.O. Box 1450
Alexandria, VA 22313-1450.

Gary J. Gershik 6/22/04
John P. White Date
Reg. No. 28,678
Gary J. Gershik
Reg. No. 39,992

Single-target molecule detection with nonbleaching multicolor optical immunolabels

Sheldon Schultz, David R. Smith, Jack J. Mock, and David A. Schultz*

Department of Physics 0319, University of California, 9500 Gilman Drive, La Jolla, CA 92093

Communicated by Harry Suhl, University of California, San Diego, La Jolla, CA, and approved November 12, 1999 (received for review September 9, 1999)

We introduce and demonstrate the use of colloidal silver plasmon-resonant particles (PRPs) as optical reporters in typical biological assays. PRPs are ultrabright, nanosized optical scatterers, which scatter light elastically and can be prepared with a scattering peak at any color in the visible spectrum. PRPs are readily observed individually with a microscope configured for dark-field microscopy, with white-light illumination of typical power. Here we illustrate the use of PRPs, surface coated with standard ligands, as target-specific labels in an *in situ* hybridization and an immunocytology assay. We propose that PRPs can replace or complement established labels, such as those based on radioactivity, fluorescence, chemiluminescence, or enzymatic/colorimetric detection that are used routinely in biochemistry, cell biology, and medical diagnostic applications. Moreover, because PRP labels are nonbleaching and bright enough to be rapidly identified and counted, an ultrasensitive assay format based on single-target molecule detection is now practical. We also present the results of a model sandwich immunoassay for goat anti-biotin antibody, in which the number of PRP labels counted in an image constitutes the measured signal.

Robust optical reporters for diagnostic detection and/or labeling are used extensively in areas of biomedical and clinical chemistry research, for instance in immunology, microbiology, molecular biology, pharmacology, pathology, virology, or drug testing. Current methods of detection use colorimetric, fluorometric, or chemiluminescent (1) reporter molecules either as enzyme substrates or as direct labels. The measured optical signal in such assays typically results from the accumulated sum of all reporter labels present in the target region, including contributions from both specific and nonspecific binding events. Alternative optical assay formats based on detecting and counting individual binding events are possible, but have not yet been demonstrated to be feasible. Although single fluorescent molecules, upconverting phosphors (2), and the recently introduced quantum dots (3, 4) can be individually detected, such systems have very low light yield and often exhibit time-dependent blinking and irreversible photodestruction. Thus, to indicate reliably the presence of a target, a population of such labels is still required, potentially limiting both the minimum quantity of target detected and the spatial localization of the labeled region.

We introduce here a new assay platform (both probe and instrumentation) capable of individual target molecule detection that uses plasmon-resonant particles (PRPs) as optical reporters. PRPs are metallic nanoparticles, typically 40–100 nm in diameter, which scatter light elastically with remarkable efficiency because of a collective resonance of the conduction electrons in the metal (i.e., the surface plasmon resonance; ref. 5). The magnitude, peak wavelength, and spectral bandwidth of the plasmon resonance associated with a nanoparticle are dependent on the particle's size, shape, and material composition, as well as the local environment. By influencing these parameters during preparation, PRPs can be formed that have a scattering peak anywhere in the visible range of the spectrum. To illustrate this capability, as well as the ability to visualize single PRPs, a color photograph (1-sec exposure time) taken of a dark-field microscope image of a red-, a green-, and a blue-colored PRP immobilized on a silicon wafer is shown in Fig. 1*A*. The scattering spectrum corresponding to each PRP is shown in Fig. 1*B*, where the peak of each spectrum has been normalized to have the same magnitude.

For spherical PRPs, both the peak scattering wavelength and scattering efficiency increase with larger radius, providing a means for producing differently colored labels. Populations of silver spheres, for example, can be reproducibly prepared for which the peak scattering wavelength is within a few nanometers of the targeted wavelength, by adjusting the final radius of the spheres during preparation. An example of a population of PRPs with nearly homogeneous scattering characteristics is shown in the microscope image of Fig. 2*A*. For very large silver spheres, the resonance width broadens appreciably, limiting the range of usable peak wavelengths to between ≈400 and ≈500 nm. To obtain PRPs that scatter at longer wavelengths (into the red spectrum), changes in other properties, such as the material or shape, can be used.

Because PRPs are so bright, yet nanosized, they can be used as indicators for single-molecule detection; that is, the presence of a bound PRP in a field of view can indicate a single binding event. As typically prepared, PRPs have a scattering cross-section of 10^{-10} cm^2; therefore, under epi-illumination (100 W halogen) with a ×100 lens (0.9 numerical aperture), a single PRP will deliver $\approx 10^7$ photons in 1 sec to the detector. Compared with other optical-labeling entities under the same illumination conditions, the ≈80-nm PRP scattering flux is equivalent to that from 5 million individual fluorescein molecules—1000-fold that provided from a 100-nm Fluosphere (Molecular Probes; data not shown) or $> 10^5$-fold that from typical quantum dots (3, 4).

PRPs, which have dimensions smaller than the wavelength of light, image as point sources under standard microscope optics, with a spatial extent determined by the aperture of the first objective lens. An intensity plot of the image of one of the PRPs in Fig. 2*A* is shown in Fig. 2*B*, as acquired by a charge-coupled device (CCD) camera located in the image plane of the microscope. The surface in the figure, known as the point spread function, represents a convolution of the ideal diffraction pattern of the PRP with the optics of the imaging system. The noticeable asymmetry in the ring pattern, for example, is related to both the illumination conditions and aberrations in the objective lens. A vertical section through the surface of Fig. 2*B* along a line of pixels passing through the center intensity maximum is plotted in Fig. 2*C*.

Although the width of the point spread function is much larger than the dimension of the actual corresponding PRP, owing to diffraction, the spatial coordinates of the PRP can be determined with much better accuracy by fitting the full two-dimensional image data set to an ideal point spread function.

Abbreviations: PRP, plasmon-resonant particle; PRISH, plasmon-resonant *in situ* hybridization; PRISA, plasmon-resonant immunosorbent assay; DD, double distilled; GAB, goat anti-biotin; RAG, rabbit anti-goat; CCD, charge-coupled device.

*To whom reprint requests should be addressed. E-mail: dschultz@ucsd.edu.

The publication costs of this article were defrayed in part by page charge payment. This article must therefore be hereby marked "*advertisement*" in accordance with 18 U.S.C. §1734 solely to indicate this fact.

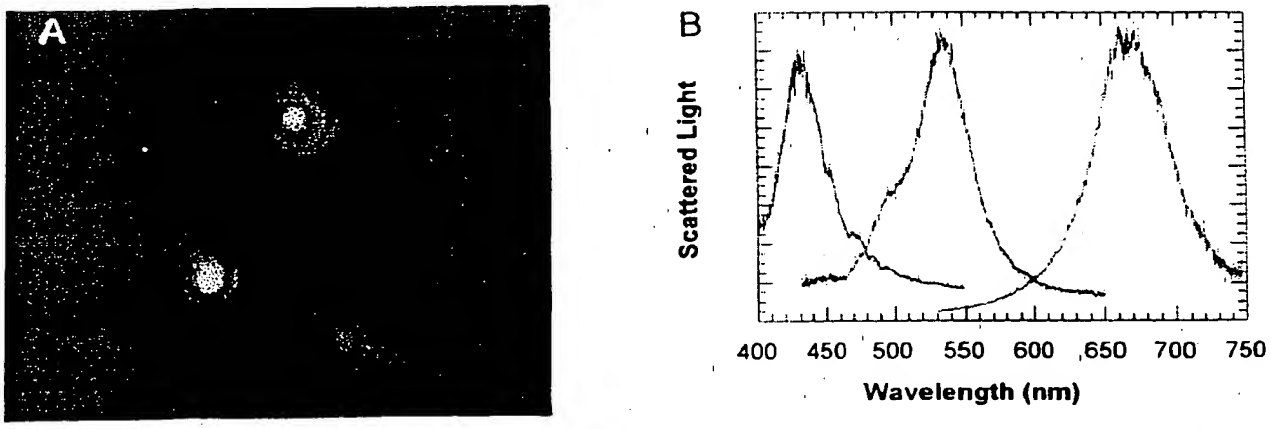

Fig. 1. (*A*) A color photograph of three PRPs illuminated with white light. The particles were chosen so that their plasmon resonance peak wavelengths would be red, green, and blue, respectively. The distance between the red and green particles is ≈4 μm. The weaker intensity of the blue PRP can be qualitatively seen by the overexposure of the film for the green and red images. (*B*) Spectral curves: the relative intensity of scattered light as a function of wavelength for the three particles shown in *A*. The two PRPs whose peak wavelengths are shifted by ≈100 nm have ≈10% overlap of intensity at the peak of their respective plasmon resonances. The full width at half height of the PRP with peak centered at ≈440 nm is ≈40 nm.

When other sources of variation are controlled, such as thermal motion or inhomogeneity in background optical index, the spatial peak of a PRP imaged by a standard CCD can be located to a precision of 10 Å. Such precision has previously been demonstrated in imaging of single fluorophores or gold nanoparticles (6). We note that, although an individual PRP can be localized with great precision, the elastic scattering from two or more PRPs of similar color cannot be separately resolved if they are located within a coherence length (roughly the wavelength of the illuminating light). Thus, for those applications requiring higher spatial resolution, PRPs of two different colors can be used.

Proteins such as antibodies can be conjugated to PRPs by techniques developed for gold colloids in light and electron microscopy, and these novel biological labels can be used in a variety of standard assays to replace less sensitive optical detection systems. Here we report on the development and use of protein-conjugated PRP reporters as labels in several exemplary biological applications.

Methods

Preparation of PRPs. For plain, uncoated PRPs (Figs. 1*A* and 2*A*), 3-nm colloidal gold nucleating cores were silver enhanced until particles of the desired size were produced. Typically, PRPs were prepared in a 20-ml vial of double-distilled (DD) water, to which 3 μl of 5-nm colloidal gold (approximate concentration, 5×10^{13} particles per ml) was added (Ted Pella, Redding, CA). The concentration of the nucleating centers used has a dramatic effect on PRP formation, not only in determining the quantity of silver required for PRP growth, but also by affecting the stability of the final colloidal solution. With a commercially available silver enhancement kit (Ted Pella), two drops of initiator (≈100 μl) was added to the solution, followed by 60 μl of silver enhancer added in 10-μl increments. The solution was continuously stirred at room temperature during the process. When the reaction was complete (after 1 or 2 min), the colloidal solution appeared a translucent yellow in transmitted light. The wavelength of the plasmon resonance for PRP samples in solution was quantitatively determined by absorbance measurements on a CARY 17D spectrophotometer. Plain PRPs were immobilized on clean glass slides or silicon wafers that were first surface treated with 0.02% alcian blue/0.5% acetic acid for 5 min, washed with DD H_2O, and air dried. The alcian blue pretreatment produces a positive charge on the slides that enhances the affinity of the negatively charged colloids for the slide surface. Silicon wafers used had a silicon dioxide layer of 100 nm and were preferred for their optical cleanliness. Samples were then rinsed in DD H_2O and dried in a compressed-air stream.

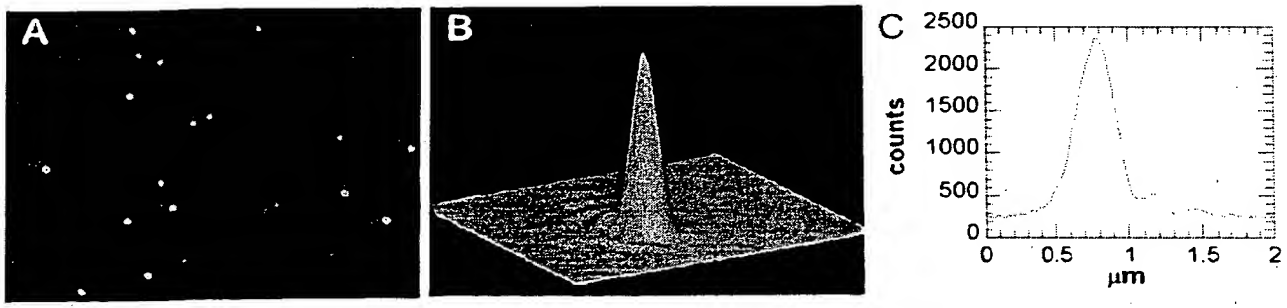

Fig. 2. (*A*) A color photograph of a collection of colloidal particles illuminated with a white light source. The area imaged is 24 × 24 μm. The particles were prepared such that their plasmon resonance peak wavelength is at ≈440 nm. (*B*) A three-dimensional–perspective CCD image of the intensity of light scattered by a single PRP. (*C*) The intensity of light measured along a line of CCD pixels passing through the maximum value of the image presented in *B*. Because the PRPs are subwavelength in size, the image of *B* is nearly that of a point source, i.e., the point spread function of the optical system. The deviations from circular symmetry are caused by asymmetry and aberrations in the objective lens.

PRP-Protein Conjugation. Conjugation of plain PRPs with proteins was carried out by procedures similar to those that have been described for conjugation of colloidal gold (ref. 7; gold colloid was purchased from BB International, Cardiff, U.K.). PRPs for the *in situ* hybridization were prepared with their resonance peak wavelength in the vicinity of 480 nm, by adjusting the amount of silver enhancer added. PRP solution (18 ml) was placed into ultraclean microcentrifuge tubes and centrifuged for 4 min at 11,750 × *g*. The supernatant was removed from the tubes, and the pellets were resuspended in 600 μl of DD H_2O. Twenty-five microliters of 100 mM sodium bicarbonate (pH 10) was added to the sample. Goat-anti-biotin [GAB (3 μg)] antibody (Pierce) was added to the PRPs, which were then incubated at room temperature with rocking. After 1 h, 100 μl of 5% BSA was added. The protein-coated PRPs were purified and separated from the excess unbound protein by centrifugation as described above. The pellet was initially resuspended in 400 μl of DD H_2O, followed by the addition of 25 μl of 10× PBS and 100 μl of 5% BSA.

For the immunoassay, 15-nm colloidal gold particles coated with rabbit anti-goat (RAG) antibody (Nanoprobes, Stony Brook, New York) were silver enhanced to produce blue PRPs. In previous work, we have found that silver enhancement of immunolabeled gold particles does not appreciably degrade the biological activity of the surface protein. Thus, preconjugated gold colloids that are themselves too small to detect visually can be silver enhanced to readily detectable PRPs. Silver enhancement can be performed before or after gold particles have been specifically bound to their target substrate.

To a 150-ml solution of 0.31% BSA, 150 μl of the 15-nm gold-RAG particles was added. While the solution was stirred, 1.75 ml of initiator was added, followed by 1.5 ml of enhancer, both added in 50-μl increments. The PRP solution was periodically spotted on slides and viewed under the dark-field microscope to monitor and control the growth of the individual PRPs. Aliquots (1 ml each) of the PRPs were spun down in ultraclean microcentrifuge tubes at 11,750 × *g* and resuspended in 20 μl of a 1:10 dilution of Tris-buffered saline/Tween (8)/0.25% BSA. The pooled fractions were used directly. The efficacy of the immunolabeled PRPs was confirmed by colorimetric tests on nitrocellulose strips spotted with various concentrations of GAB antibody.

PRP Detection and Analysis. All imaging was performed with a Nikon Optiphot microscope that had a CF Plan BD ×100, 0.9 numerical-aperture objective lens. Digital, monochrome images were acquired with a Photometrics CH200 CCD camera (KAF1400 chip) mounted on the trinocular port of the microscope head. To obtain plasmon resonance curves from individual PRPs, light was redirected via a beam splitter to an image-plane aperture (0.2-mm diameter), followed by an optical fiber centered on the optic axis. An ocular focused on the aperture was used to position PRPs into the center of the aperture. Light collected by the fiber was then transmitted into an SPEX 270M grating spectrometer, to which the Photometrics CCD camera could be mounted. The wavelength dependence of the source, optics, and CCD was removed by normalizing the spectra to the spectra obtained from a broad-band light-scattering target (Labsphere, North Sutton, New Hampshire).

***In Situ* Hybridization.** The polytene chromosome "squashes" were prepared by Seashell Technology (San Diego) as described (8). DNA encoding the white (*w*) gene genomic region was isolated from *Drosophila* chromosomal DNA by PCR amplification. Biotin-modified nucleotides were incorporated either by PCR amplification or by random priming (High Prime Biotin; Roche Molecular Biochemicals). The DNA probe was purified and concentrated by using Nuctrap columns (Stratagene) and ethanol precipitation. After hybridization with 100–300 ng of denatured-probe DNA in hybridization buffer [0.6 M sodium chloride/2× Denhardt's solution (0.02% polyvinylpyrrolidone/0.02% Ficoll/0.02% BSA)/10 mM magnesium chloride/20% dextran sulfate/100 mM sodium phosphate, pH 6.8] at 68°C for 21 h, the squashes were washed with 2× SSC at 60°C for 45 min. Before incubation with GAB PRPs for 1 h, the slides were washed with 0.5× PBS. Nonbound PRPs were removed by washing with DD H_2O.

The PRP-labeled chromosomes were stained with a 1:10,000 dilution of SYBR Green (Molecular Probes) nucleic acid gel stain solution made up in 1× PBS and placed under a coverslip. The stained and labeled chromosomes were photographed under dark-field illumination with a 75-W xenon light source. No filters were used, either in excitation or emission.

Cytological Assay. For the immunohistochemical assay, 2- to 3-μm sections of frozen chick intercostal muscle tissue were prepared as previously reported (9, 10) and transferred to either glass microscope slides for optical imaging or transmission electron microscope grids for imaging in the electron microscope. After mounting, the tissue (in all of the samples) was washed 3× for 5–10 min in PBS, then blocked for 20 min (3% normal goat serum/1% immunogold silver staining-grade gelatin/0.01% Triton X-100), and washed again for 5 min in a 1:3 dilution of PBS. After incubation with a 1:5 dilution of anti-ryanodine receptor 34C primary antibody for 1 h at room temperature, the samples were washed six times for 3–5 min each time in PBS. Next each sample was incubated with 5-nm gold colloid coated with goat anti-mouse antibody (Nanoprobes) that was diluted 1:40 in DD H_2O. The sample was then washed six times in PBS, with each wash lasting 3–5 min.

Samples on slides for optical characterization were then silver enhanced with a gelatin enhancer solution and carefully monitored, and the enhancing reaction was quenched by washing with DD H_2O when individual PRPs were visible. The gelatin enhancer solution was prepared, immediately before use, by adding 50 μl of initiator and 50 μl of enhancer to 1 ml of a 2-mg/ml gelatin solution. The gelatin solution was prepared by adding the gelatin to DD H_2O and heating to boiling temperature. The gelatin enhancer solution was placed onto the DD H_2O-rinsed chicken muscle sections for 8 min and then rinsed away.

Immunoassay. The test immunoassay was performed in the "sandwich" format. The lid of a standard 48-well dish (Corning Costar) was incubated overnight with a solution of 0.2-mg/ml biotinylated BSA (Pierce) in 100 mM sodium bicarbonate (pH 10) at room temperature. The lids, which had distinct regions indicated by raised plastic circles, were used rather than the plates themselves because the wells are too deep to allow imaging with the microscope objectives that are available. Excess, nonbound biotinylated BSA was removed by washing. Various amounts of GAB antibody (ranging from 0.06 to 10,000 pg), in 50 μl of PBS containing 0.25% BSA were incubated in the plastic wells of the lids overnight. The plastic wells were then rinsed with 0.5× PBS. In the final step, each well was incubated with 50 μl of the RAG-PRP solution, prepared as described above, for 1 h. Unbound PRPs were removed by washing with DD H_2O.

Results and Discussion

We performed three routine biological assays with antibody-coated PRPs substituted for other commonly used optical labels. All of the optical microscopic images were taken under dark-field illumination, by using a 75-W xenon arc source (see above) without any filters. In all cases, incubations or growth steps were allowed to progress just long enough that individual PRPs could still be identified, rather than allowing numerous PRPs to cluster and form aggregates. In principle, a PRP assay has single-

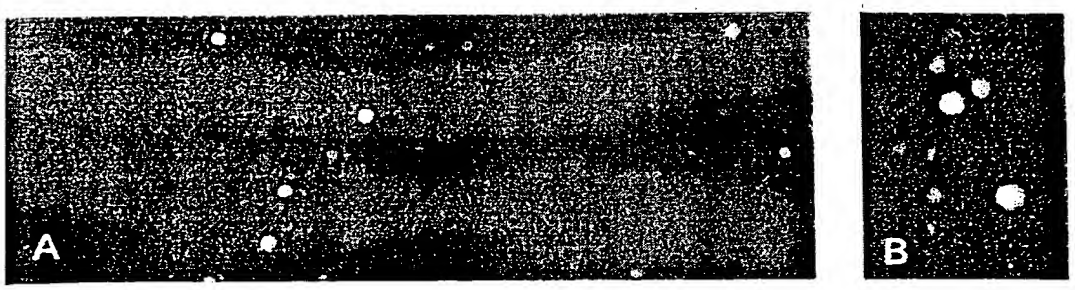

Fig. 3. Photographs of the region of the *Drosophila* X chromosome (band 3C) specifically labeled with colloidally prepared blue PRPs via the *in situ* hybridization protocol described in *Methods*. The typical distance between PRPs is ≈2 μm. The polytene chromosome is counterstained with SYBR Green. Both the SYBR Green fluorescence, and the light scattered by the PRPs are photographed simultaneously. The large number of parallel aligned copies of DNA present in the polytene chromosome provides multiple target sites for PRP hybridization, suitable for illustrative purposes, but excessive for the counting of individual PRPs for quantitative analysis. (*A*) The region of the white gene (*w*) from the tip of the X chromosome, with band 3C PRP labeled. (*B*) A close-up of the 3C band from another sample, illustrating the large density of PRPs that can be clustered yet still be readily identified as individual target site labels.

molecule sensitivity, although the relative amount of specific to nonspecific binding, the equilibrium-binding constant, and the density of target molecules set the practical limits to this sensitivity. The length of incubation time is also a factor in the signal, because each individual binding event can provide an observable change in signal. Rather than reaching equilibrium binding conditions, some signal may be sacrificed to allow for incubations that are very short compared with typical assays.

In our experiments, traditional blocking procedures adapted from protocols for assays with other labels were used without further optimization. Even so, background binding was very low (at most, several PRPs per field of view), except in some tissue areas that had high levels of background PRP binding. We believe that electrostatic interactions play a significant role in this nonspecific binding, and we are currently investigating methods for reducing this background.

The first biological assay we present here, which was performed with PRP labels, is a modification of DNA *in situ* hybridization. Nucleic acid *in situ* hybridization is a widely used biological diagnostic assay that requires sensitive reporter labels. In a typical DNA fluorescence *in situ* hybridization experiment (FISH), for example, fluorescent reporter labels are attached to nucleic acids that bind to a targeted genomic locus (11, 12). Owing to the low inherent detection sensitivity of individual fluorescent reporter molecules, amplification steps are generally needed in fluorescence *in situ* hybridization to produce a measurable signal. Such amplification techniques result in a loss of spatial information as the amplification material builds up and/or diffuses around the site being probed. In a DNA *in situ* hybridization, this loss of information limits the minimum number of bases that can be resolved between pairs of markers.

We chose to demonstrate PRP *in situ* hybridization (PRISH; Seashell Technology) by using the polytene chromosome isolated from the salivary glands of a *Drosophila* larva. In these chromosomes, ≈1000 identical DNA copies of the genome are aligned in parallel. The specific gene chosen as the target was the white gene (*w*) located near the tip of the X chromosome (band 3C; ref. 13).

The microscope image in Fig. 3 shows the tip of a SYBR Green-stained X chromosome from a *Drosophila* polytene chromosome squash after hybridization with the biotinylated *w* gene DNA probe and labeling with GAB antibody-coated PRPs. Dark-field illumination was used, with no further fluorescence filtering, so that both the chromosome and PRPs could be observed simultaneously. The typical distance between PRPs is ≈2 μm. The natural banding pattern present in the polytene chromosome allowed for visualization, identification, and confirmation of the specific site of chromosome labeling.

In Fig. 3, PRPs can be seen labeling the 3C band on the chromosome. These particles could be individually visualized after the primary hybridization. No additional amplification steps were used to enhance the signal. In fact, although the multiple, parallel aligned copies of the *Drosophila* genome available in the polytene chromosome were convenient for demonstration purposes, this density of target is not required from the standpoint of PRP labeling. Efforts are currently underway to perform the analogous experiment of labeling a human chromosome. By using two or more sets of PRPs that have different colors and surface ligands, simultaneous identification and positioning of multiple, different nucleic acid probes should be possible for DNA-mapping applications.

The second biological assay demonstrating PRP capability is a modification of immunohistochemistry in a mounted tissue sample. This assay illustrates the flexibility of the PRP-labeling system because, in samples that are resistant to penetration by entities as large as fully grown PRPs, assays can be performed with labeled colloidal gold as the probe. After gold labeling, silver enhancement can be performed, just long enough to produce visually detectable, precisely localized, individual PRPs, rather than the traditional large, dark silver masses used by light microscopists performing immunogold silver staining (7). Protein-conjugated colloidal gold particles can be obtained commercially in sizes ranging from 1 nm to hundreds of nanometers. In labeling of tissue samples for electron microscopy, for example, the smaller-sized immunogold particles (<10 nm) are preferred because of improved tissue accessibility.

To illustrate the efficacy of developing PRPs from immunogold bound to specific tissue-labeling sites in a sample, we targeted ryanodine receptors found in chicken skeletal muscle. In longitudinal sections of skeletal-muscle tissue, the ryanodine receptors are found at the triadic junctions between the sarcoplasmic reticulum and transverse tubule system. Ryanodine receptor immunoreactivity is found at the junctions of the sarcoplasmic reticulum and transverse tubule system, which are present along the *z* lines (9, 10, 14).

A color photograph of an optical dark-field image of the PRP-labeled (silver-enhanced) tissue is shown in Fig. 4*A*. The single arrow in the figure indicates a row of four bound PRPs, an intensity line plot of which is shown in Fig. 4*B*. The average spacing between PRPs, as measured from the figure, corresponds to 0.5 ± 0.05 μm, in agreement with that observed by electron microscopy.

To confirm the targeted site labeling, some of the ultrathin cryosections were prepared on transmission electron microscopic grids and labeled, as shown in the electron micrograph in Fig. 4*C*. This and other electron micrographs reveal the PRPs as

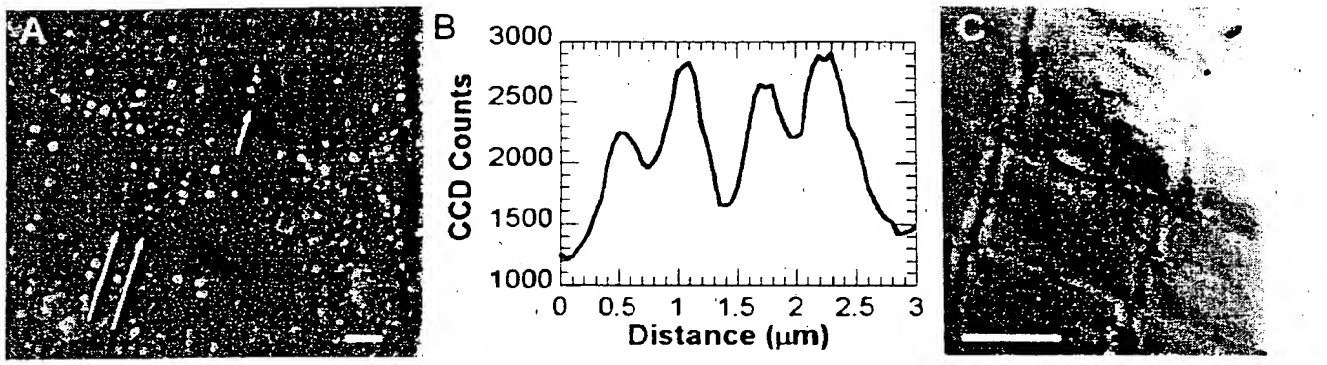

Fig. 4. (*A*) A color photograph of a chicken muscle tissue section in which the ryanodine receptors have been immunogold labeled, and then silver enhanced until individual PRPs have been formed. The optical microscope configuration and detection system is similar to that used for the data of Fig. 2. The white arrows indicate the direction of the parallel set of *z* lines located between the lines of PRPs. (Bar = 2 μm.) (*B*) An intensity (count) line scan along the direction indicated by the single arrow in *A*, demonstrating that the individual PRP image peaks are readily resolved. (*C*) A transmission electron micrograph of a tissue section similar to that used for *A*, confirming that the PRPs are found along the *z* lines in a latticelike fashion characteristic of the known spatial distribution of ryanodine receptors at the sarcoplasmic reticulum and transverse tubule system junctions. (Bar = 1 μm.)

black dots located at the triadic junctions of the sarcoplasmic reticulum and transverse tubule system. Typically, from one to five colloidal particles labeled a junction, with the junctions forming a more-or-less regular lattice of sites spaced 0.5 μm apart on average. Concentrations of initiator and silver enhancer were found, along with appropriate incubation times, which resulted in the formation of individual silver nanoparticles nucleated from the immunogold cores. If an excess of silver enhancer was used or the reaction proceeded for too long, then the nucleated silver would form large clumps of material, losing the spatial resolution.

As is well known, the electron microscope provides unparalleled spatial localization and allows visualization of (nonlabeled) features in the stained tissue. The sample preparation and observation, however, must be compatible with a vacuum environment. In the example shown above, PRPs detected by a normal light microscope allow the positions of the ryanodine receptor sites to be located optically. Moreover, the samples were successfully imaged in buffer underneath a coverslip, indicating that, *in vitro* and likely *in vivo*, real-time kinetic assays are possible with PRP labeling.

In a third example of a PRP-modified assay, we investigated the use of PRPs for quantification of target molecules in a counting-based assay in the equivalent of a "sandwich" ELISA. The ELISA, the traditional assay to determine the presence or concentration of a target molecule in a sample, typically uses labeled antibodies that bind specifically to the target. The resulting signal, for example fluorescent or colorimetric, is proportional to the sum of all reporter labels present in the sample, including those specifically bound to the target molecule as well as those from nonspecific background binding. ELISA samples are usually prepared in standard multiwell dishes and analyzed by measuring the optical density of the incubation solution (1). By contrast, in the PRP-based immunosorbent assay (PRISA; Seashell Technology), the measured signal is the numerical count of all PRPs bound to the target molecules and immobilized on the plate. Although this method can be expected to saturate at a very dense concentration of target molecules, counting individual PRPs should lead to very high sensitivity in samples with very low concentrations of target.

The results from the sandwich PRISA are shown in Fig. 5. In this test assay, a polystyrene lid from a 48-well dish, surface coated with biotinylated BSA, served as the capture substrate. Samples of GAB antibody (constituting the target), in amounts ranging from 0 (control, dark horizontal line) to 600 pg, were added into the lid wells and allowed to incubate overnight. The GAB antibody was then detected with RAG antibody-labeled PRPs. The PRPs present in the various wells, corresponding to a range of GAB antibody ("target") concentrations, were counted, and, as seen in Fig. 5, the signal covered over four orders of magnitude in concentration. A minimum detection sensitivity of ≈60 fg was achieved.

The level of sensitivity achieved in the PRISA is on a par with the most sensitive commercial assay kits. Immunosorbent assays based on PRP detection, however, have a potential advantage over alternative detection formats because the ideal assay volumes are submicroliter, sparing precious sample. Moreover, by miniaturizing the area of the capture surface, increased detection sensitivity should be realized. The individual target molecule detection provided by PRP labeling allows for this miniaturization of immunoassays, a feature important for applications such as ultra-high-throughput screening, as in combinatorial drug libraries, or DNA microarrays for functional genomics studies (15–18).

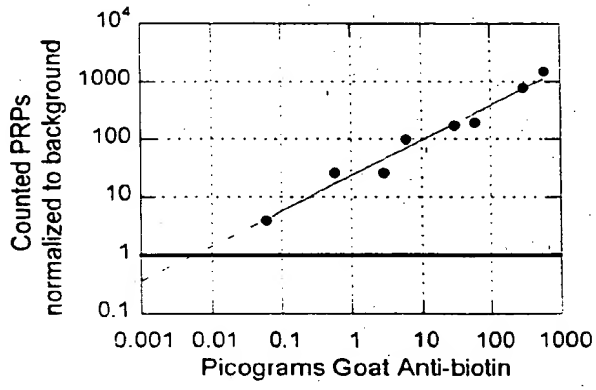

Fig. 5. Results of a PRP-based immunoassay. In this test assay, a polystyrene surface coated with biotinylated BSA served as the reaction substrate. After blocking this surface with nonbiotinylated BSA, a dilution series of GAB antibody (constituting the target), in amounts ranging from 0 (control) to 600 pg, was added and allowed to incubate overnight. After a wash step, PRPs conjugated with RAG antibodies were then incubated with the samples for 1 h, after which the samples were washed, air dried, and imaged.

The PRP-based biological assays reported here demonstrate how commonly used labels such as fluorophores can be replaced (as in the PRISA) or complemented (as in the PRISH) by PRPs. The preferred probe depends on the scattering properties of the target, as well as the quantity of material being probed. PRPs, being elastic scatterers, do not have the benefit of rejecting incident light that is scattered from the sample, as do fluorescent probes; however, in our work we have found that scattered light from PRPs can easily be discriminated from that arising from tissue or other background (e.g., Figs. 3 or 4). When the light scattered from the sample is excessive, algorithms based on recognition of the characteristic point spread function of a PRP can be used to identify the PRP and reject the background scattering.

Further studies are required to achieve the full capabilities of single-molecule detection that PRP labels provide and to demonstrate their effectiveness in the design of novel biosensors (19–22). The methodologies reported here allow for the development of many different types of assay formats. For example, one could bind PRPs to a surface via linker molecules that are susceptible to cleavage by exogenously added molecules, such as enzymes. The progressive release of the bound particles from the surface would be a measure of the amount of enzyme activity.

The results presented here, combined with the recent studies of Raman scattering from molecules surface adsorbed to PRPs (23), may result in novel biological labels and chemical sensors. In addition, the ability to localize and resolve PRPs to the precision described may also find important applications in metrology and nanotechnology (24).

We acknowledge with appreciation the preparation of the tissue section used in Fig. 4 by Professor Mark Ellisman and members of the National Center for Microscopy Imaging Research, Tom Deerinck, Victoria Edelman, and Ying Jones. We thank James Bouwer, Genalyn Rocha, and Matt Pufall at the University of California, San Diego for technical assistance and Dr. Beth Friedman of Seashell Technology (San Diego) for samples of polytene chromosomes. We thank Professors R. Doolittle, G. Feher, M. Ellisman, P. Saltman, G. Fortes, and Dr. S. L. McQuaid for critical reading of the manuscript. PRP, PRISA, and PRISH are trademarks of Seashell Technology. This research was supported by National Science Foundation Grants DMR 96–12252, 96–23949, and 97–24535; National Institutes of Health Grants 1R21HG01959–01 and 1R43HG01597; and the Richard Lounsbery Foundation.

1. Kricka, L. J., ed. (1995) *Nonisotopic Probing, Blotting, and Sequencing* (Academic, San Diego), 2nd Ed.
2. Faris, G. W., Wright, W. H., Pati, S., Schneider, L. V. & Zarling, D. A. (1996) in *OSA Trends in Optics and Photonics: Biomedical Optical Spectroscopy and Diagnostics*, eds. Sevick-Muraca, E. & Benaron, D. (Optical Soc. Am., Washington, DC), Vol. 3, pp. 225–228.
3. Warren, C. W. & Nie, S. (1998) *Science* **281**, 2016–2018.
4. Bruchez, M., Moronne, M., Gin, P., Weiss, S. & Alivisatos, A. P. (1998) *Science* **281**, 2013–2015.
5. Schultz, S., Mock, J., Smith, D. R. & Schultz, D. A. (1999) *J. Clin. Ligand Assay* **22**, 214–216.
6. Denk, W. & Webb, W. W. (1990) *Appl. Opt.* **29**, 2382–2391.
7. Hayat, M. A., ed. (1989) *Colloidal Gold: Principles, Methods and Applications* (Academic, San Diego), Vols. I, II, and III.
8. Sambrook J., Fritsch, E. G. & Maniatis, T., eds. (1989) *Molecular Cloning* (Cold Spring Harbor Lab., Plainview, NY), 2nd Ed., p B.14.
9. Lim, J. K. (1993) *Dros. Inf. Serv.* **72**, 73–77.
10. Airey, J. A., Beck, C. F., Tanksley, S. J., Deerinck, T. J., Ellisman, M. H. & Sutko, J. L. (1990) *J. Biol. Chem.* **265**, 14187–14194.
11. Sutko, J. L., Airey, J. A., Murakami, K., Takeda, M., Beck, C., Deerinck, T. & Ellisman, M. H. (1991) *J. Cell Biol.* **113**, 793–803.
12. Barch, M. J., ed. (1991) *The ACT Cytogenetics Laboratory Manual* (Raven, New York), 2nd Ed.
13. Lindsley, D. L. & Zimm, G. G., eds. (1992) *The Genome of Drosophila melanogaster* (Academic, San Diego).
14. Bloom, W. & Fawcett, D. W. (1968) *A Textbook of Histology* (Saunders, Philadelphia), 9th Ed.
15. Hieter, P. & Boguski, M. (1997) *Science* **278**, 601–602.
16. Rowen, L., Mahairas, G. & Hood, L. (1997) *Science* **278**, 605–607.
17. Fodor, S. P. A. (1997) *Science* **277**, 393.
18. Goffeau, A. (1997) *Nature (London)* **385**, 202–203.
19. Elghanian, R., Storhoff, J. J., Mucic, R. C., Letsinger, R. L. & Mirkin, C. A. (1997) *Science* **277**, 1078–1081.
20. Holtz, J. H. & Asher, S. A. (1997) *Nature (London)* **389**, 829–832.
21. Lin, V. S. Y., Motesharei, K., Dancil, K. P., Sailor, M. J. & Ghadiri, M. R. (1997) *Science* **278**, 840–843.
22. Gupta, V. K., Skaife, J. J., Dubrovsky, T. B. & Abbott, N. L. (1998) *Science* **279**, 2077–2080.
23. Nie, S. & Emory, S. R. (1997) *Science* **275**, 1102–1106.
24. Silva, T. J., Schultz, S. & Weller, D. (1994) *Appl. Phys. Lett.* **65**, 658–660.